Supplementary Information (SI) for Journal of Materials Chemistry A.
This journal is © The Royal Society of Chemistry 2026

Supporting information

for

Floatable Ionic Photothermal Aerogels for Water and Energy Harvesting Under Solar Light

Bibek Chaw pattnayak,[a] Piyusaranjan Giri,[b] Upasana Mohapatro,[a] Madhurima Jana,[b] Sasmita Mohapatra*[ac]

[a]*Applied Nanomaterials Research Laboratory, Department of Chemistry, National Institute of Technology, Rourkela, Odisha-769008, INDIA*

[b]*Molecular simulation laboratory, Department of Chemistry, National Institute of Technology, Rourkela, Odisha-769008, INDIA*

[c]*Centre for Nanomaterials, National Institute of Technology, Rourkela, Odisha-769008, INDIA*

*Corresponding author: Tel: 91-661-2462661, Fax: 91-661-2472050,

*E-mail: sasmitam@nitrkl.ac.in

i. Characterization:

Morphology and microstructure of SCPC hydrogel evaporators were analyzed by using the Scanning electron microscopy (SEM) (JEOL JSM- 6480 LV). Various crystallographic planes of the materials were studied using an X-ray diffractometer (XRD) (Bruker AXS D8 Advance). The surface functional units of the synthesized materials and hydrogels were analyzed using Fourier-transform infrared spectroscopy (FTIR) (IRAffinity-1S, Shimadzu). Molecular morphology characterization of photothermal material and various water states of hydrogels was studied using a PL micro-Raman spectrometer (Witec Alpha300, Germany). The IR images and surface temperatures were captured by a Testo 868 IR thermal imaging camera. The concentrations of various ions were studied by using ICP-OES (inductively coupled plasma optical emission spectroscopy). The percentage of absorbance, transmittance, and reflectance was characterised using UV-Vis-NIR spectrophotometer (Agilent Cary 5000). The absorbance of the samples was analysed by using UV-Vis spectrophotometer (Shimadzu UV-2600). The intensity of sunlight was measured by using Metravi 207 solar power meter. A Xenon lamp of 300 W of intensity 1 $kW \cdot m^{-2}$ was used as a solar simulator. The open-circuit voltage was measured and recorded using a digital multimeter (Meco-81-USB)

ii. Thermal conductivity measurement

The thermal conductivities of the wet and dry SCPCs were calculated by using the "sandwich method".[1] The wet and dry SCPCs were sandwiched between two slides of glass and placed on a heating platform. Basically, there are three interacting interfaces present in the system. The first surface is between the bottom glass slide and the heating platform (T_1), the second one lies between the bottom glass and SCPC (T_2) and the third one is between the SCPC and the top glass (T_3). All the interface temperatures were monitored by using a thermal camera and a thermocouple. The heat transfer rate (q) was obtained by the following Fourier formulae-

$$q = -k1\frac{T2 - T1}{d1} = -k1\frac{dT}{dx}$$

Where k_1 is the thermal conductivity of the glass slide (1.05 W m^{-1} k^{-1}) and d_1 represents the thickness (10 mm) of the glass slide. Then, by using the transfer rate of heat and the temperature difference, the value of thermal conductivities of wet and dry SCPCs was calculated by the following equation-

$$k = -q\frac{d2}{T3 - T2} \quad (2)$$

where d_2 and k represent the thickness and thermal conductivity of the RSEs, respectively.

iii. **Heat loss analysis**

The heat loss of the SCPC evaporator mainly consists of three components - radiation, convection, and conduction.

The detailed calculations are illustrated below.

(1) Radiation

The radiation heat loss is calculated according to the Stefan-Boltzmann law:

$$E_{\text{radiation}} = \varepsilon\,(T^4{}_{\text{SCPC}} - T^4{}_{\text{environment}}) \quad (3)$$

Where $E_{\text{radiation}}$ denotes radiation heat flux, ε represents the emissivity (in this study is assumed as 0.93), and σ is the Stefan-Boltzmann constant (5.67×10^{-8} W m^{-2} K^{-4}). T_{SCPC} and $T_{\text{environment}}$ are the steady-state surface temperature (63 **ºC**) of the photothermal evaporator under solar

light irradiation and ambient temperature (25 **°C**) under 1 kW m^{-2} solar light irradiation for 0.5 h, respectively. Therefore, the radiation heat flux is calculated to be 261 W m^{-2}.

Hence, the radiation heat loss can be calculated by the following equation:

$$\eta_{radiation} = E_{radiation} / E_{all} \quad (4)$$

Based on equation 6, we can calculate that the radiation heat loss of the device accounts for ~26.1 % of all irradiation energy.

(2) Convection

The convection heat loss is calculated by Newton's law:

$$E_{convection} = Ah\,(T_{RSE} - T_{environment}) \quad (5)$$

Where $E_{convection}$ shows the convection heat flux, A and h represent the surface area (60 cm^2) of the RSE evaporator and convection heat transfer coefficient (about 5 W m^{-2} K^{-1}), respectively. Therefore, the radiation heat loss can be calculated by the following equation.

$$\eta_{convection} = \frac{E_{convection}}{AE_{all}} = \frac{h(T_{RSE} - T_{environment})}{E_{all}} \quad (6)$$

Based on equation-8, we can calculate that the convection heat loss of the device accounts for ~19 % of all irradiation energy.

(3) Conduction

The radiation heat loss is calculated according to the following equation:

$$E_{conduction} = Cm \triangle T \quad (7)$$

Where $E_{\text{conduction}}$ denotes the conduction heat flux, C is the specific heat capacity of water (4.2 J g^{-1} C^{-1}), m is the water weight (100 g), and $\triangle T$ (3 ˚C) is the temperature change of bulk water before and after solar light irradiation for 0.5 h under 1 kW m^{-2} solar light irradiation.

Then, the radiation heat loss can be calculated by the equation:

$$\eta_{conduction} = \frac{E_{conduction}}{AE_{all}} \quad (8)$$

Based on equation-10, we can calculate that the conduction heat loss of the device accounts for ~2.1% of all irradiation energy.

iv. Estimation of energy consumption by dark experiment:

By following the literature method of our recent publication, the vaporisation enthalpy of the evaporator can be calculated as follows. Water and SCPC evaporator having the same evaporation area were placed in a lab-made container. The mass change under the dark condition was calculated to evaluate the vaporisation enthalpy of the water present in the hydrogel evaporator using the following equation:

$$U = E_e M_p = E_0 M_0 \quad (9)$$

where M_0 represents the change in mass of the bulk water without having the hydrogel evaporator, E_0 is the vaporisation enthalpy of the bulk water under the dark condition, and M_p is the change in mass of the SCPC evaporator in the same condition. The vaporisation enthalpy (E_e) could be evaluated by making the comparison with the theoretically derived known value of the water (2450 J/g). The calculated average values were obtained to calculate the energy efficiency (Table S1).

v. Calculation of energy consumption by DSC measurement-

The measured vaporisation enthalpy of the bulk water was calculated to be 2340 J/g, which is quite close to the calculated theoretical value of 2445 J/g, demonstrating a good measurement with accuracy. The obtained values from the DSC are little higher than that of the values obtained from the dark evaporation experiment, because the DSC calculation represent complete dehydration of SCPC, evaporating all states of water including free water (FW), bound water (BW), and intermediate water (IW), whereas in dark experiments only FW and IW have been considered.

vi. **Evaluation of Solar-to-vapor conversion efficiency of RSE:**

The solar-to-vapor conversion efficiency is calculated by using the following formula:

$$\eta = m\,h / P_t \qquad (10)$$

Where 'm' represents the mass change i.e., mass flux, 'h' represents the liquid to vapour phase change enthalpy and P_t represents the power density of sunlight on the evaporator interface.

For SCPC, m= 2.9 – 0.1 = 2.8 kg m^{-2} h^{-1}, h = 1250 J/g. Therefore, the solar-vapor conversion efficiency of SCPC was estimated to be 97% under the solar irradiation of one sun.

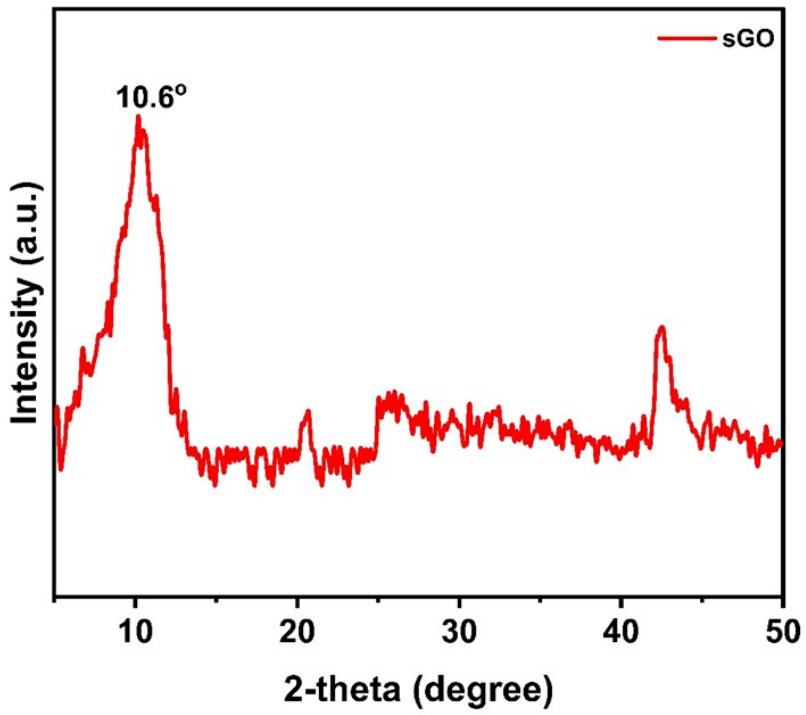

Figure S1. XRD pattern of sGO. The characteristic peak at 2θ = 10.6° confirmed the successful formation of GO from graphite powder.

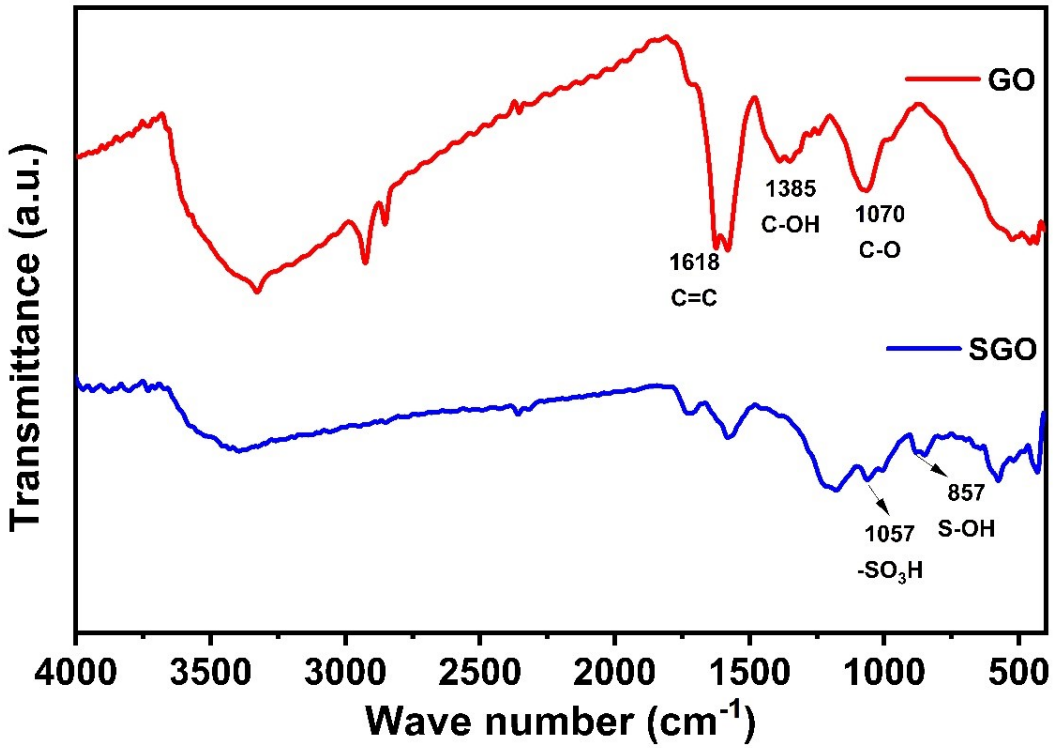

Figure S2. FTIR spectra of GO and sGO. The peaks at 1070, 1385, and 1618 is attributed to the presence of C-O, C-OH, and C=C of the graphene oxide (GO). The peaks at 857, and 1057 are assigned to the presence of S-OH and SO_3H groups of sGO respectively, which confirms the successful sulphonation of GO.[2]

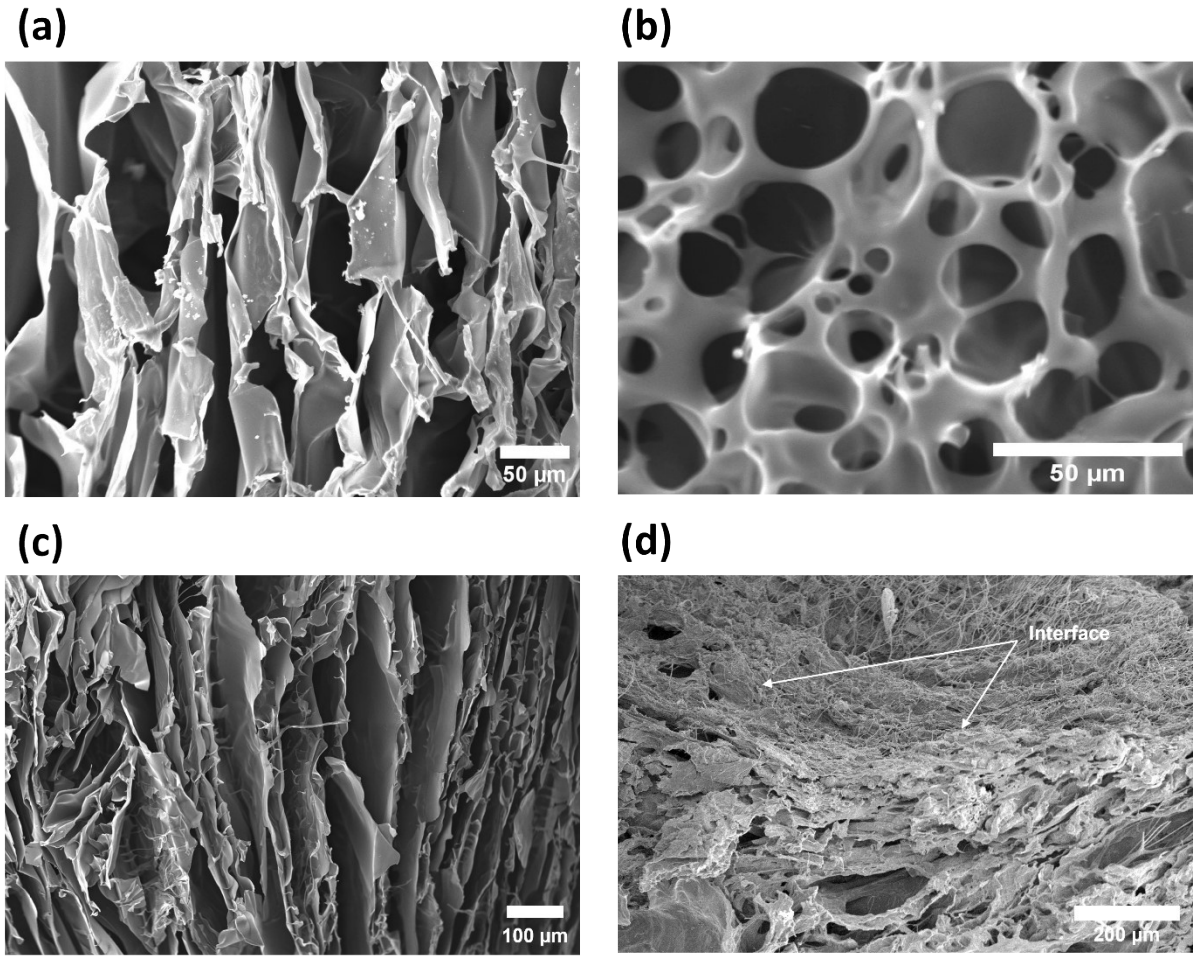

Figure S3. SEM images of bottom photothermal layer of SCPC evaporator (c) longitudinal view, (b) cross-sectional view and (c,d) cross-sectional interface between the top photothermal layer and bottom water transport layer.

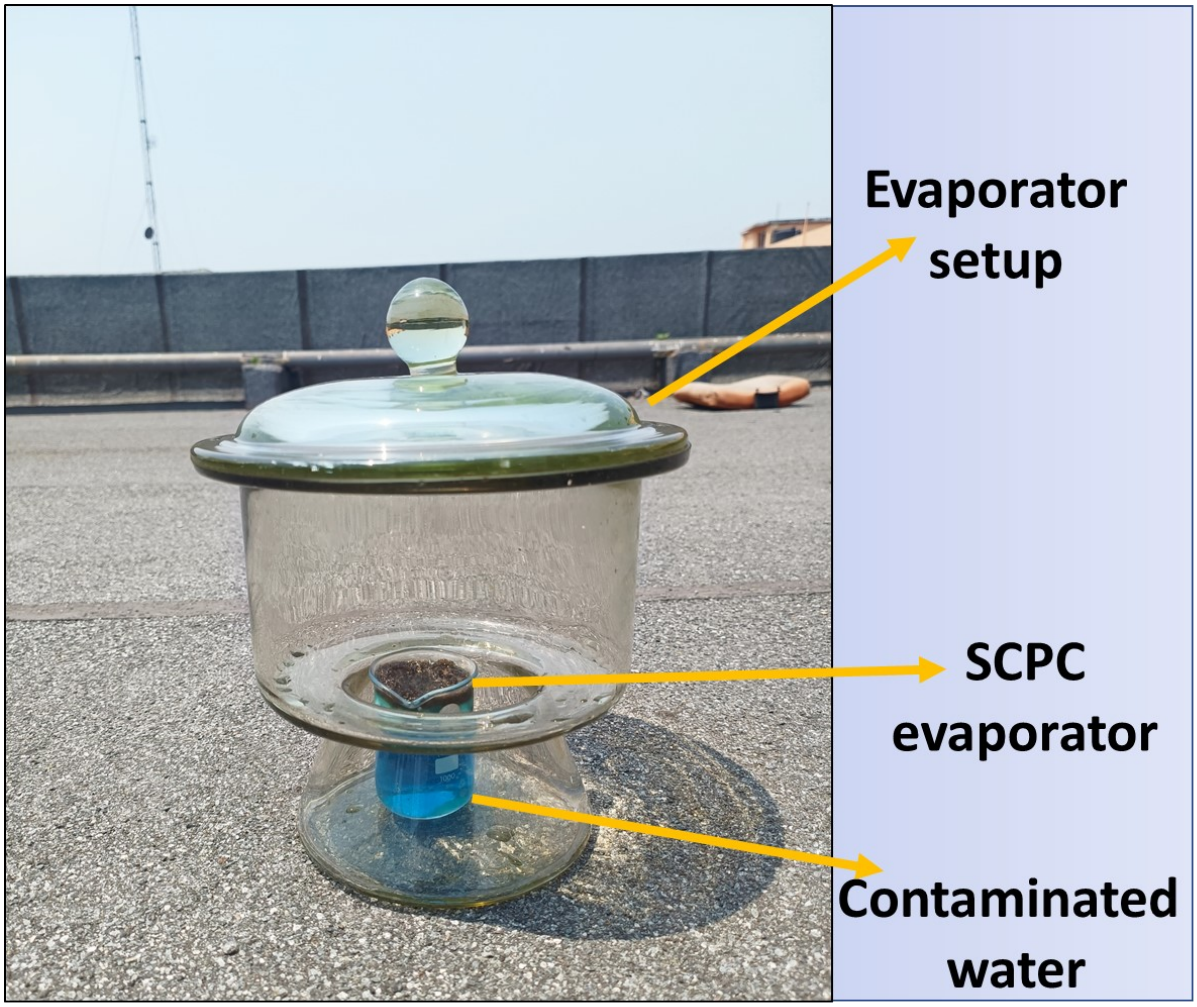

Figure S4. SCPC evaporator setup.

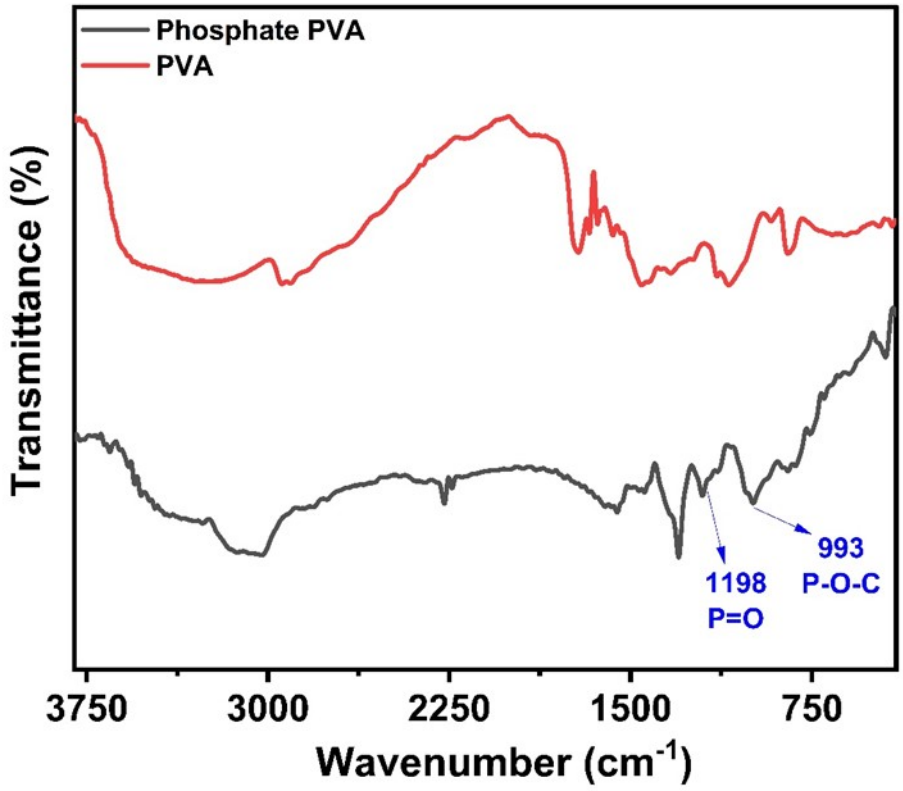

Figure S5. 1198 cm^{-1} is attributed to the functional unit P-O-C and P=O, which confirms the successful phosphorylation of PVA.[3]

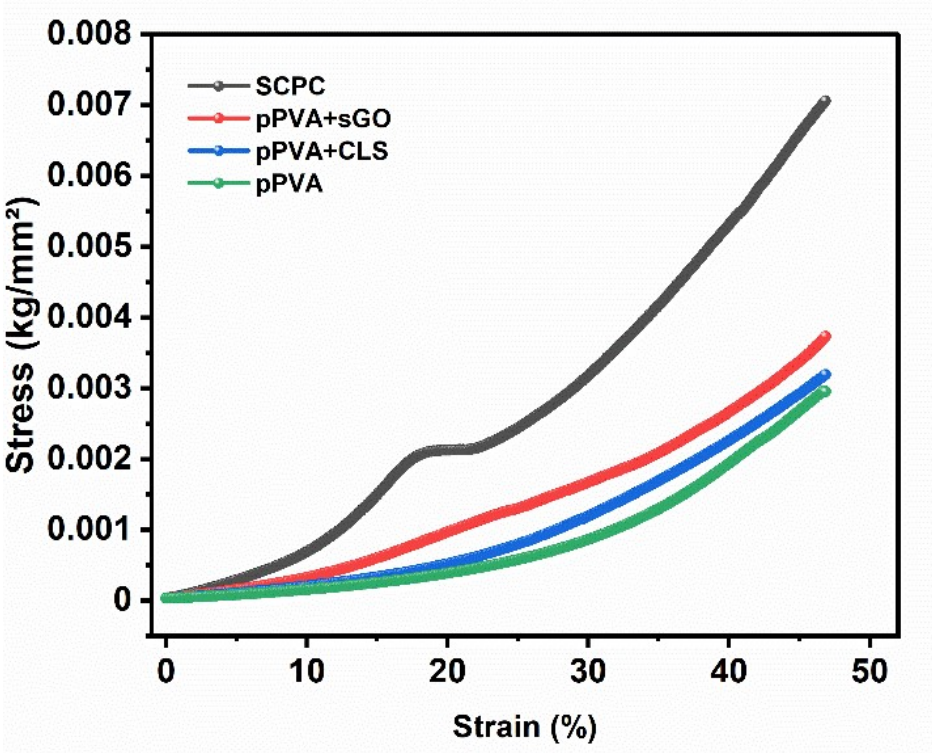

Figure S6. Tensile stress-strain curve for different hydrogels.

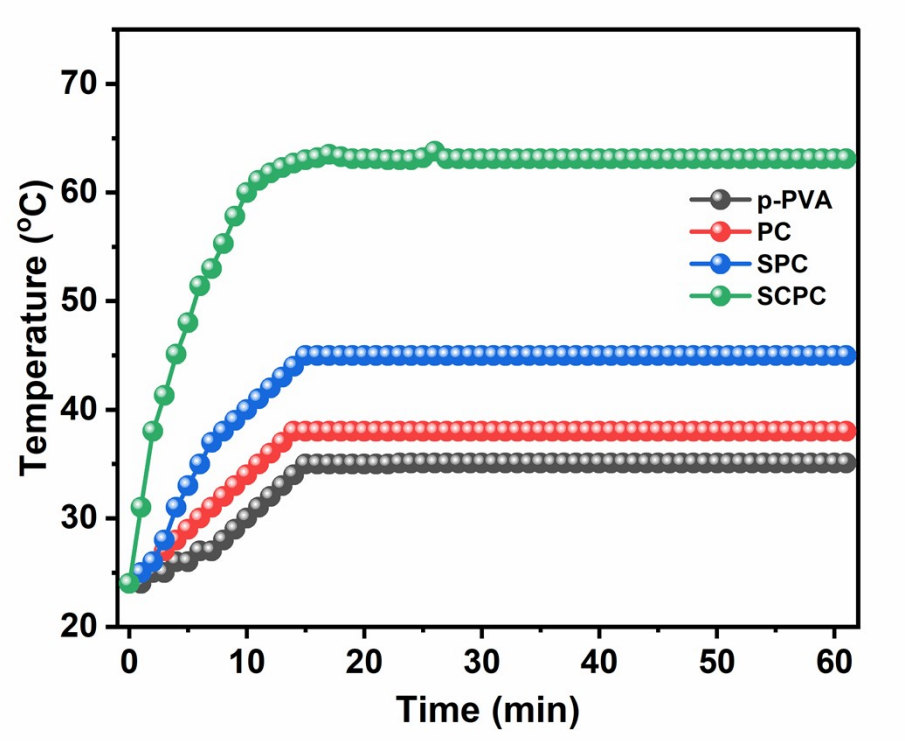

Figure S7. Temp. vs time plot for different hydrogels.

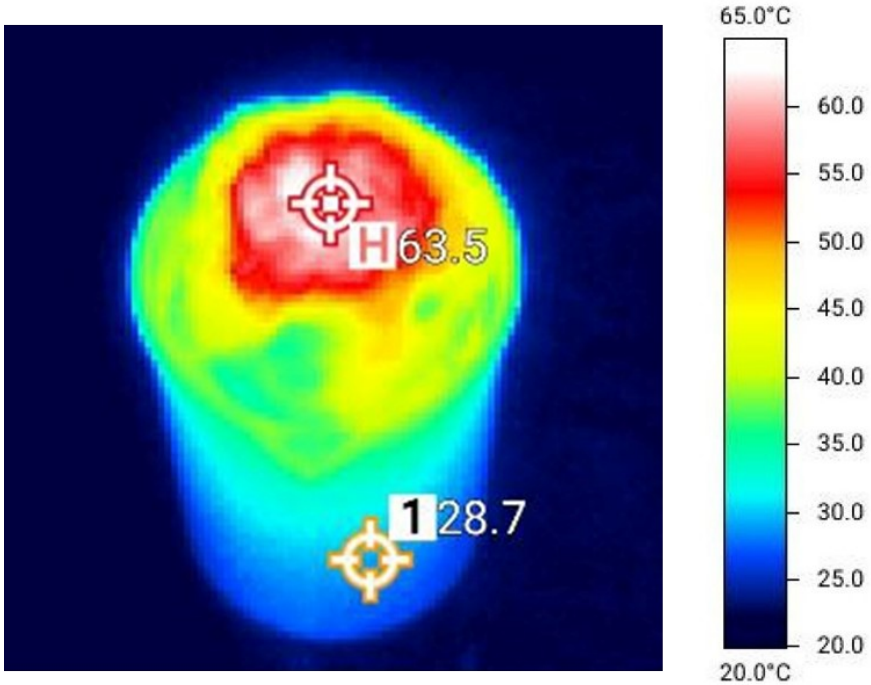

Figure S8. Side view of the SCPC evaporator under the solar irradiation of one sun.

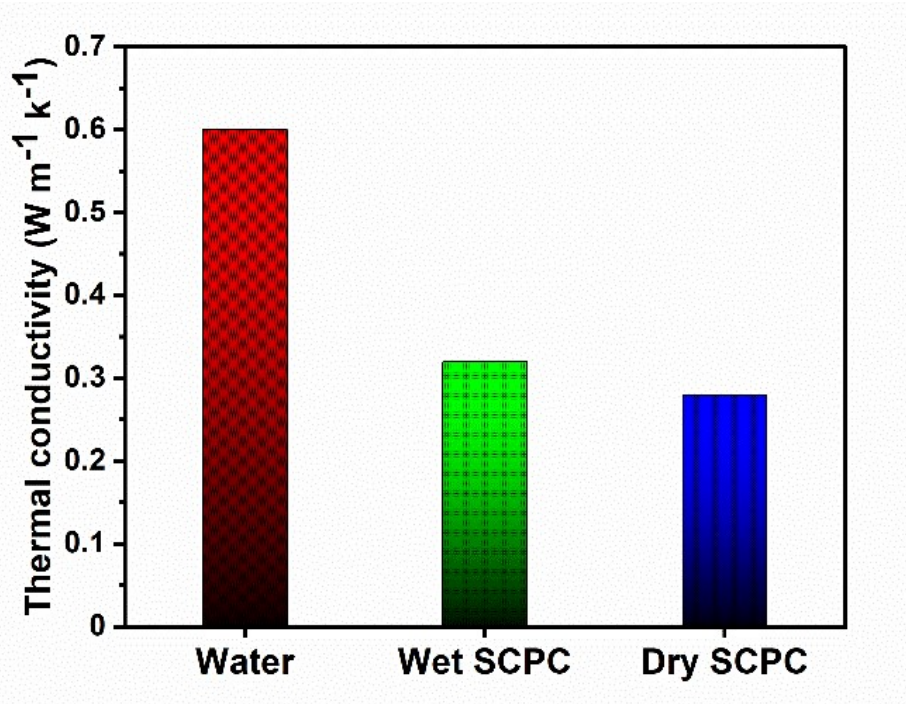

Figure S9. Thermal conductivity of water and SCPC evaporator in wet state and dry state.

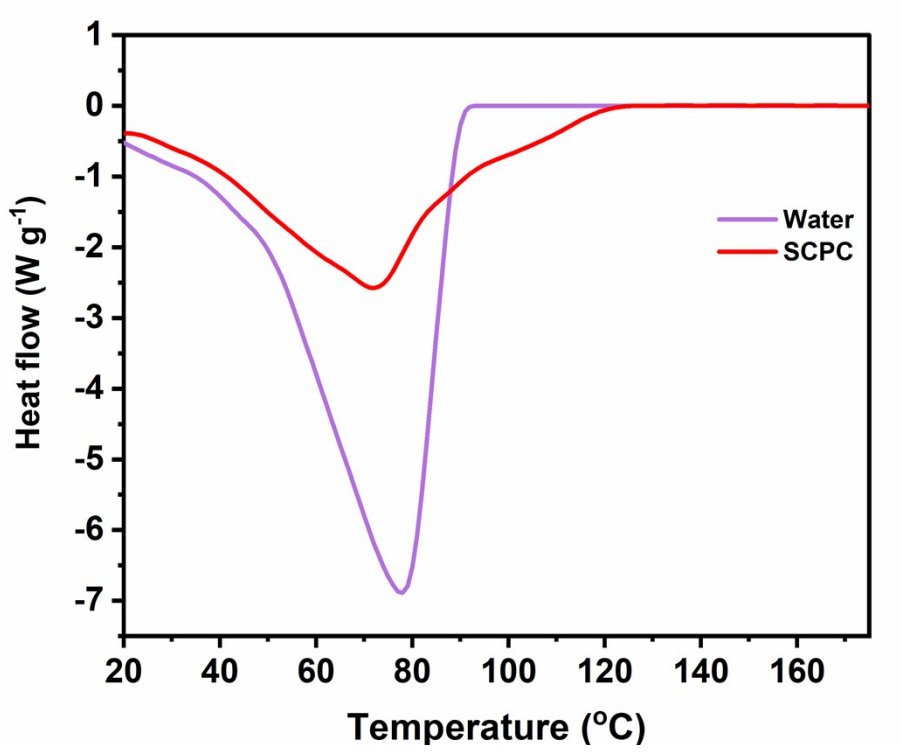

Figure S10. Thermograms of SCPC evaporators and water.

Table S1. Comparison of energy consumption obtained from dark experiment and DSC measurement.

Energy consumption (J/g)	Water	SCPC
DSC measurement	2340	1356
Dark experiment	-	1250

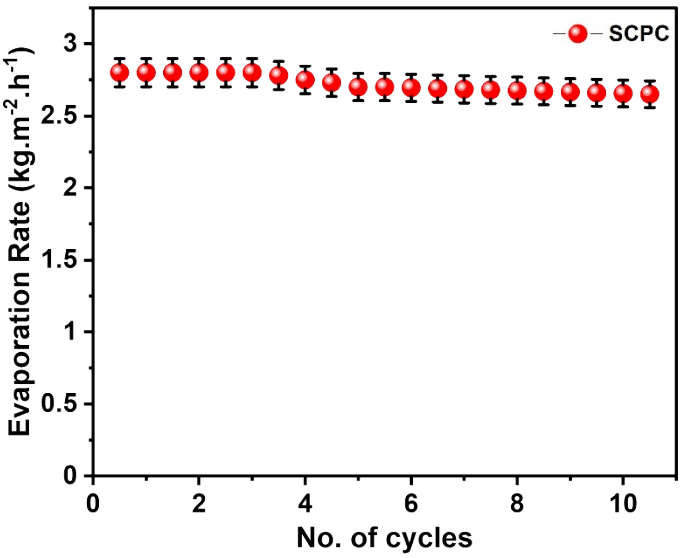

Figure S11. Steam generation rate of SCPC evaporator with different no of cycles.

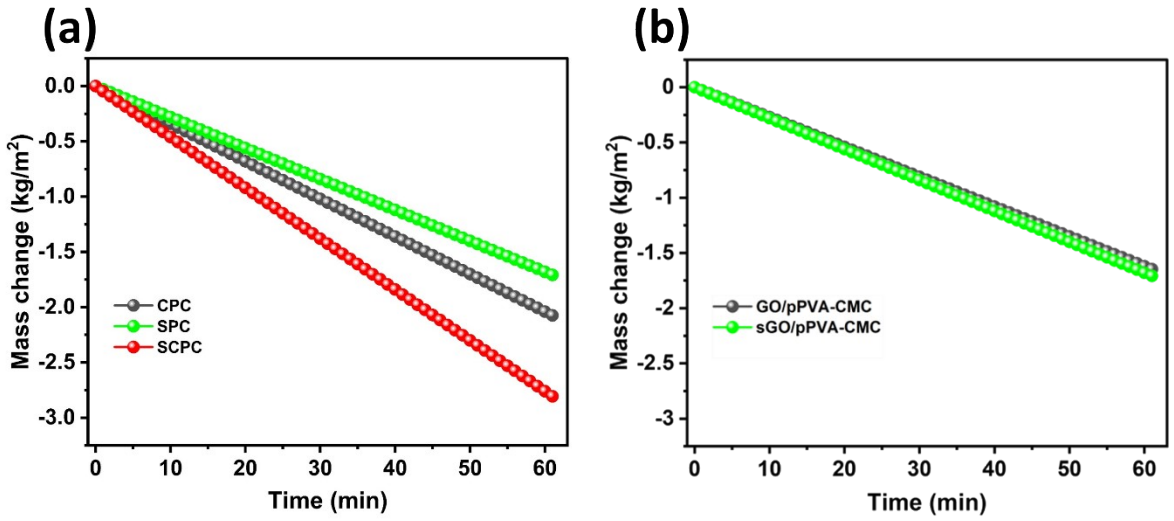

Figure S12. (a) Mass change Vs time plot for CPC, SPC, and SCPC evaporator and (b) hydrogels using GO and sGO.

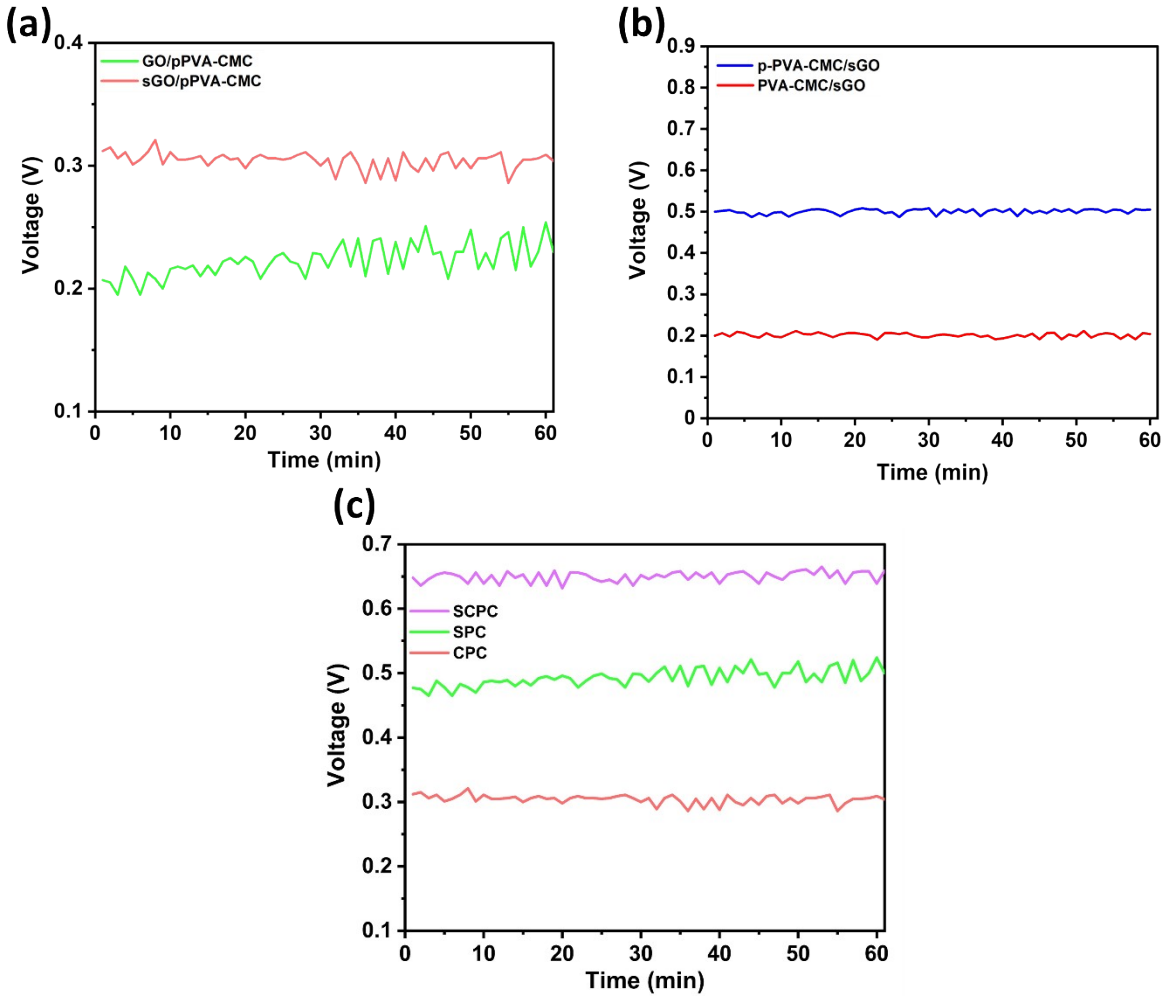

Figure S13. Voltage Vs time plot for (a) hydrogels with GO Vs sGO, (b) hydrogels with PVA Vs p-PVA and (c) CPC, SPC, and SCPC evaporators.

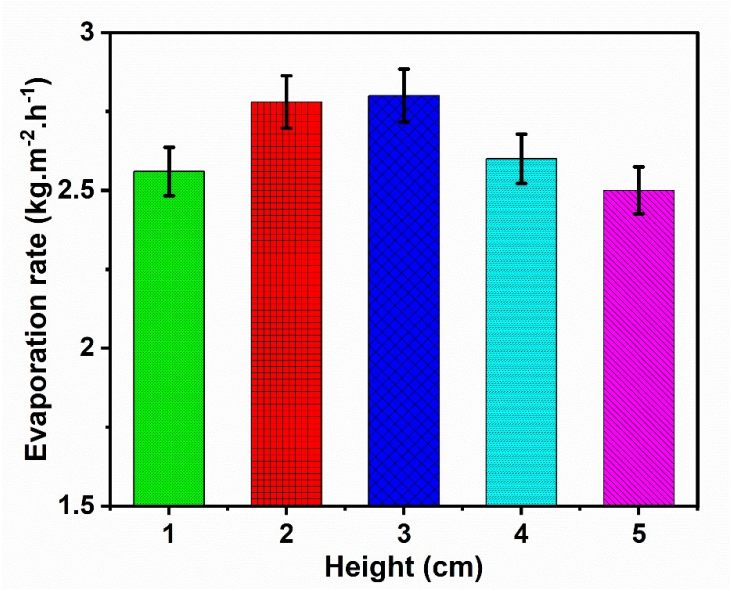

Figure.S14. Variation of evaporation rate with increase in height of the SCPC evaporator.

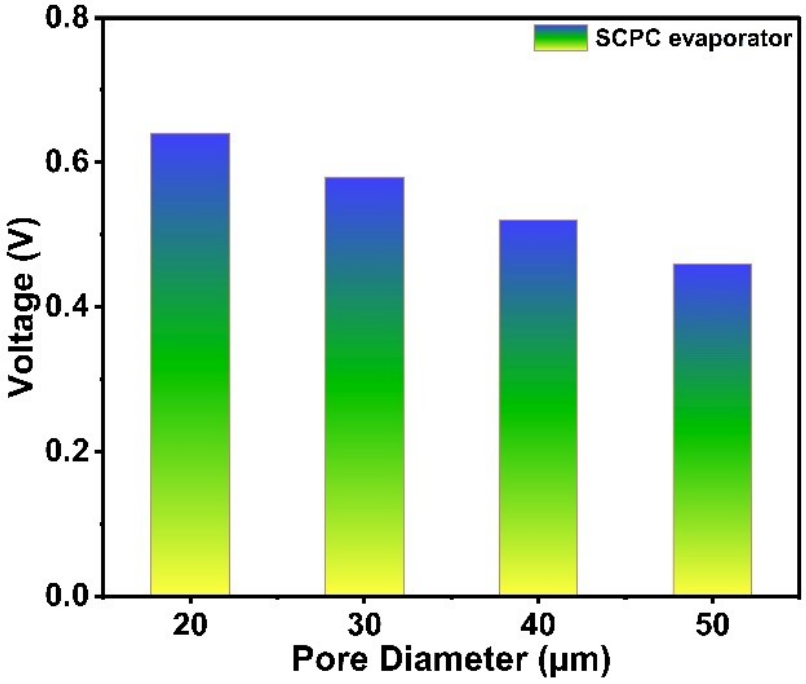

Figure S15. Voltage vs pore size plot for SCPC evaporator.

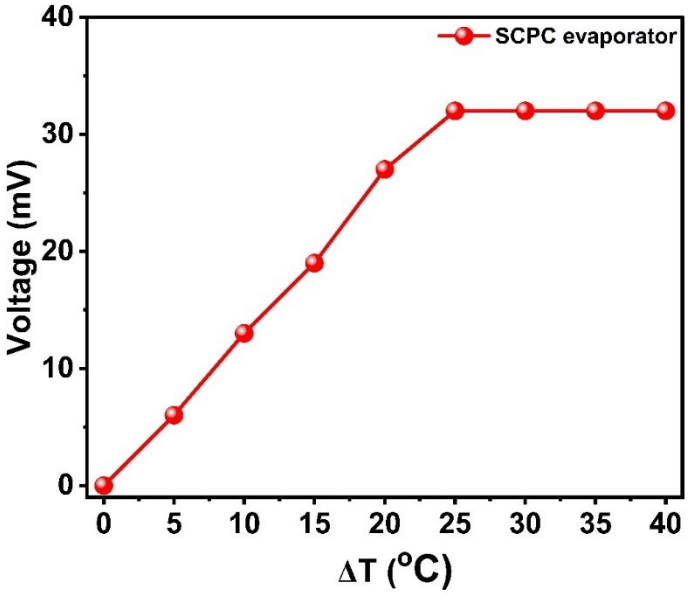

Figure S16. Voltage vs temp difference plot for SCPC evaporator.

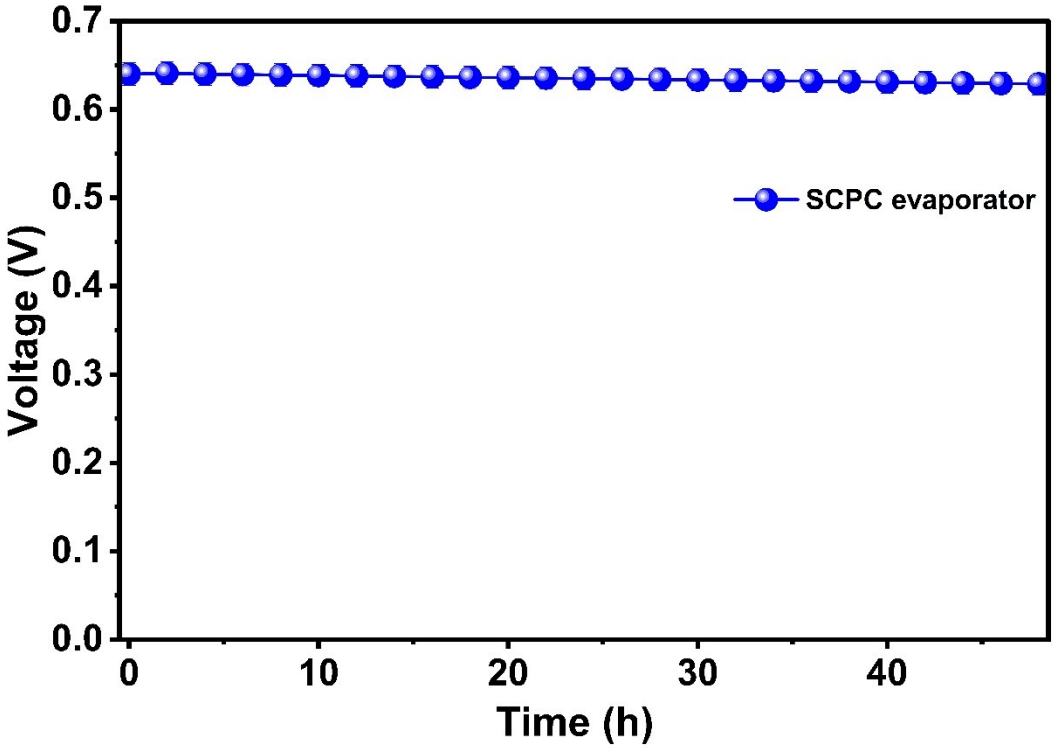

Figure S17. Voltage vs time plot for SCPC evaporator.

Molecular Dynamics Simulation Methodology

Two different systems, consisting of the anionic form of four PVA molecules (FigureS12), henceforth denoted as '*a*PVA', 40 hydrogen ions (H^+), and water molecules were taken in two different cubic simulation boxes of edge length ~ 20 Å and 35 Å, containing 267 and 1430 water molecules, respectively, to perform atomistic molecular dynamics (MD) simulation. The systems with edge lengths of ~ 20 Å and 35 Å are henceforth designated as S1 and S2, respectively. It is worth noting that the S2 system was obtained by diluting the S1 system 1.5 times. After system preparation, energy minimization was performed using the steepest-descent algorithm in GROMACS 5.1.4 with the GROMOS force-field version 54A7.[1,2] The systems were subsequently heated for 1 ns, followed by 2 ns of equilibration under NPT conditions and an additional 2 ns under NVT conditions. Production simulations were then carried out for 100 ns in the NPT ensemble, and the trajectories were saved every 0.5 ps for subsequent analysis. During the simulations, the temperature and pressure were regulated using the Nosé-Hoover thermostat[3] and the Parrinello-Rahman barostat,[4] respectively, with periodic boundary conditions applied in all directions. Particle Mesh Ewald (PME) method[5] was used to compute long-range electrostatic interactions. A cutoff distance of 12 Å was used for neighbor lists and van der Waals interactions. All the bond lengths were constrained using the LINCS algorithm.[6,7] The equations of motion were integrated with a 1 fs time step.

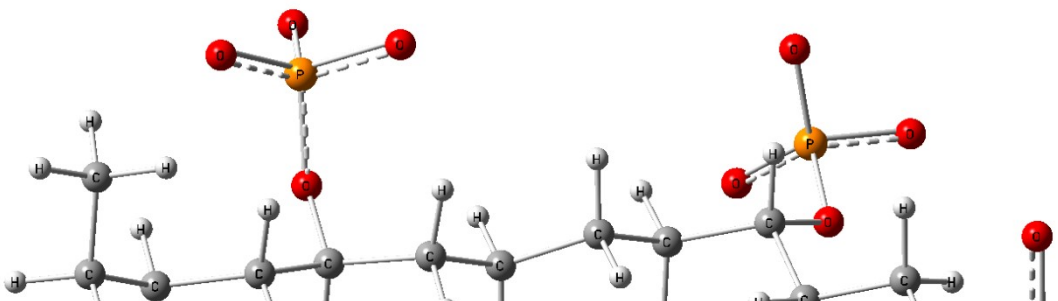

Figure S18. Atomic configurations of PVA phosphate (*a*PVA)

Table S2. Evaporation and electricity generation study of different hydro-voltaic generators.

Evaporators	**Evaporation rate (kg m^{-2} h^{-1}) (Under one sun)**	**Voltage (V)**	**Current (μA)**	**Power Density (μW cm^{-2})**	**Reference**
MXene cotton fabric	1.38	0.363	2.2	0.80	4
Carbon black/PVDF membrane	1.44	0.32	1.5	0.48	5
Biochar/PAAm hydrogel	2.22	0.016	0.008	0.00013	6
PSS@CNT/rGO	1.85	0.46	-	-	7
CNT-rGO@Ni foam	1.37	0.5	10	5	8
SCPC	2.8	0.64	480	307.2	This work

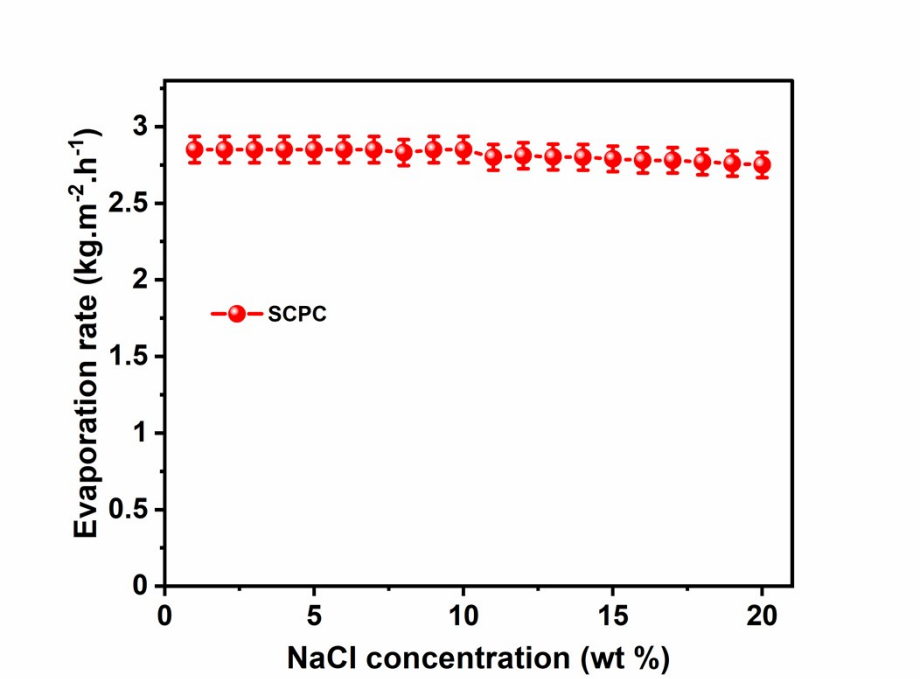

Figure S19. Evaporation rate of SCPC evaporator at different salt concentrations under the solar irradiation of one sun.

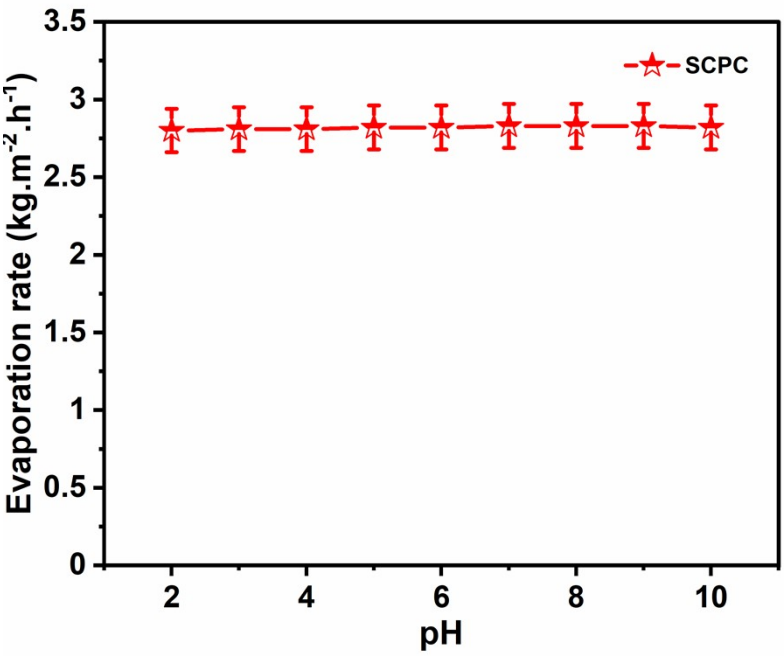

Figure S20. Evaporation rates of SCPC evaporator at different pH.

References.

1. X. Liu, D. D. Mishra, Y. Li, L. Gao, H. Peng, L. Zhang and C. Hu, *ACS Sustainable Chemistry & Engineering*, 2021, **9**, 4571-4582.
2. I. K. Basha, E. M. Abd El-Monaem, R. E. Khalifa, A. M. Omer and A. S. Eltaweil, *Scientific Reports*, 2022, **12**, 9339.
3. J. Xie, R. Lv, H. Peng, J. Fan, Q. Tao, Y. Dai, Z. Zhang, X. Cao and Y. Liu, *Journal of Radioanalytical and Nuclear Chemistry*, 2020, **326**, 475-486.
4. H. Peng, D. Wang and S. Fu, *ACS Applied Materials & Interfaces*, 2021, **13**, 38405-38415.
5. Y. Xu, S. Dong, Y. Sheng, C. Liu, F. Xing, Y. Di and Z. Gan, *Journal of Materials Chemistry A*, 2023, **11**, 1866-1876.
6. R. Tarek, D. A. Kospa, S. El-Hakam, A. I. Ahmed and A. A. Ibrahim, *Desalination*, 2023, **566**, 116935.
7. Y. Wu, H. Huang, W. Zhou, C. You, H. Ye, J. Chen, S. Zang, J. Yun, X. Chen and L. Wang, *ACS Applied Materials & Interfaces*, 2022, **14**, 29099-29110.
8. Z. Chen, X. Li, R. Liu, K. Ma, H. Sang, Y. Huang and C. Tang, *Industrial & Engineering Chemistry Research*, 2022, **61**, 16565-16576.